Ignition And Burning Rate Characteristics Of Pyrolant Black Powder

Takuo Kuwahara

Department of Aerospace Engineering, College of Science and Technology
Nihon University, 7-24-1 Narashinodai, Funabashi City, Chiba 274-8501, Japan
E-mail: tkuwahara@aero.cst.nihon-u.ac.jp

Abstract: *Composite propellants contain binder as fuel which connects oxidizer particles and metals. The burning rate of a propellant is affected by the concentration and type of binder. Pyrolant is mixed with oxidizer particles and metal particles. Pyrolant does not contain binder, so burns smoothly. The burning rate of black powder (BP) which is a kind of pyrolant is higher than that of AP composite propellant. The shorter the reaction time in the gas phase near the burning surface of black powder becomes, the higher the burning rate becomes. The burning rate of BP is inversely proportional to the ignition delay time.*

Keywords: *Black powder, pyrolant, ignition delay time, burning rate*

Introduction

Pyrolant consists of mixed oxidizer particles and metal particles. Oxidizers such as ammonium dinitramide (ADN), ammonium perchlorate (AP), ammonium nitrate (AN), hydrazinium nitroformate (HNF), potassium nitrate (KN), cyclotrimethylene trinitramine (RDX), etc. are used. Metals such as aluminum (Al), boron (B), magnesium (Mg), titanium (Ti), zirconium (Zr), etc. are used. Several kinds of pyrolants are used for pyrotechnics, as gas generator, ignition material, heat supply, etc.

These particles are electrified and easily ignited by static electricity. The sensitivity of a pyrolant is generally high. The ignition delay time of a pyrolant is shorter than that of an AP composite propellant. The burning rate of a pyrolant is easily controlled by changing the concentration of oxidizer.[1–5]

There are two types of pyrolants. One type burns homogeneously, oxidizer and fuel melt at the burning surface and it is easy to evaluate the burning mechanism. The burning rate of black powder (BP) is not changed by the sizes of potassium nitrate (KNO_3), charcoal (C), and sulfur (S). Black powder belongs to this homogeneous type. The other type burns heterogeneously, not melting at the burning surface and the burning rate changes when the size of the compositions changes, as Mg/TF, B/KNO_3 and it is difficult to evaluate the burning mechanism.

We used black powder in this study. Standard compositions were KNO_3/C/S = 75/15/10 wt%. Charcoal was made from pine. By changing the concentration of these materials, the burning rate was controlled. We studied the combustion wave structure near the burning surface with small thermocouples, and the relationship between burning rate and ignition delay time.

Theoretical investigation

(1) Heat balance at burning surface

The burning rate, r, is defined by the following equation:[6,7]

$$r\rho_{\mathrm{p}}\{C_{\mathrm{p}}(T_{\mathrm{s}}-T_0)-Q_{\mathrm{s}}\} = \lambda_{\mathrm{g}}\Phi_{\mathrm{s}^+} = \lambda_{\mathrm{g}}\frac{T_{\mathrm{f}}-T_{\mathrm{s}}}{\delta} \tag{1}$$

$$\delta = u_{\mathrm{g}}(\tau_{\mathrm{pb}}+\tau_{\mathrm{cb}}) = \frac{r\rho_{\mathrm{p}}}{\rho_{\mathrm{g}}}(\tau_{\mathrm{pb}}+\tau_{\mathrm{cb}}) = \frac{r\rho_{\mathrm{p}}RT_{\mathrm{f}}}{P_{\mathrm{g}}}(\tau_{\mathrm{pb}}+\tau_{\mathrm{cb}}) \tag{2}$$

In equation (2), we use the mass balance equation, and equation of state,

$$r\rho_p = u_g\rho_g$$

$$\rho_g = \frac{P_g}{RT_g}$$

$$u_g = \frac{r\rho_p}{\rho_g} = \frac{r\rho_p RT_f}{P_g} \quad (3)$$

where ρ_p = density of pyrolant, C_p = specific heat capacity, T_s = surface temperature, T_0 = initial temperature, Q_s = heat of reaction at the surface, λ_g = heat conductivity in the gas phase, Φ_{s+} = temperature gradient near the burning surface in the gas phase, T_f = flame temperature, δ = reaction length, u_g = gas velocity, τ_{pb} = physical process time, as mixing and diffusion, τ_{cb} = chemical reaction time, ρ_g = gas density, R = gas constant, and P_g = pressure. The adiabatic flame temperature T_f is calculated with NASA-CEA.[8] In this study P_g = 0.1 MPa, ρ_p, C_p, and R are constant. If T_s and Q_s are constant, the burning rate will be obtained following equation (4):

$$r^2 = \alpha\frac{T_f - T_s}{T_f(\tau_{pb} + \tau_{cb})} = \alpha\frac{1 - \frac{T_s}{T_f}}{\tau_{pb} + \tau_{cb}} \quad (4)$$

where α is a constant. If $T_s < T_f$ and $\tau_{pb} = 0$, equation (4) will become

$$r^2 = \alpha\frac{1}{\tau_{cb}} \quad (5)$$

The burning rate is determined by the chemical reaction time. This chemical reaction time is obtained from equation (6):

$$\tau_{cb} = Z_{sb}\exp(\frac{E_{sb}}{T_{sb}R}) \quad (6)$$

where Z_{sb} is a constant and E_{sb} is the activation energy of the pyrolant. T_{sb} is obtained following equation (7):

$$T_{sb} = \frac{T_f + T_s}{2} \quad (7)$$

where T_f is the flame temperature and T_s is the temperature of the burning surface.

(2) Ignition characteristics

The surface temperature of the pyrolant increases with passing time when pyrolant is put into the furnace, and reaches decomposition temperature, and gas is generated at the surface of the pyrolant. The generated gas reacts near the surface and heat is conducted from the reaction gas to the surface. A luminous flame appears and the pyrolant ignites. Ignition delay time τ_{ig} can be separated into two terms, the first of which is physical delay time τ_p, which is the time to reach the pyrolant decomposition temperature, and the second is the chemical delay time τ_c, which is the time from decomposition to appearance of a luminous flame. The ignition delay time is obtained following equation (8):

$$\tau_{ig} = \tau_p + \tau_c \quad (8)$$

τ_{ig} is measured experimentally, and the physical delay time τ_p is defined as the minimum ignition delay time. The chemical delay time is obtained following equation (9):

$$\tau_c = \tau_{ig} - \tau_p \quad (9)$$

The chemical ignition delay time τ_c is the same as the chemical reaction time τ_{cb} of equation (6).

$$\tau_c = Z_s\exp(\frac{E_s}{T_sR}) \quad (10)$$

The decomposition gas reacts in the gas phase near the burning surface when it burns or ignites, therefore $Z_s = Z_{sb}$, $E_s = E_{sb}$, and $T_s = T_{sb}$. If physical ignition delay time $\tau_p < \tau_c$, we will obtain the following equation:

$$2\log(\frac{1}{r}) \propto \log(\tau_{cb}) \approx \log(\tau_c) \approx \log(\tau_{ig}) \quad (11)$$

Burning rate is inversely proportional to ignition delay time.

Experimental

(1) Thermal decomposition

The thermal decomposition characteristics were obtained with thermo-gravimetric (TG) and differential thermal analysis (DTA). The heat of reaction at the surface (Q_s) was measured using differential scanning calorimetry (DSC). These experiments were conducted in N_2 gas atmosphere at 0.1 MPa and the N_2 gas flow rate was 50 ml min^{-1}. The heating rate was 10 K min^{-1}

and the sample mass was 3 mg for TG, DTA and DSC experiments. The mean diameter of KNO_3 particles was 30 μm, that of S was 30 μm, and that of C was 10 μm.

(2) Burning rate

To investigate the effect of sulfur on burning rates, the burning rate was measured with varying concentrations of sulfur in an atmosphere at 0.1 MPa, with a KNO_3/C ratio of 75/15. The concentration of oxidizer was changed and the effect of oxidizer on burning rate was measured, with C/S = 15/10. The pellet was 10 mm in diameter and 10 mm in length and cigarette burning type was used. The burning rate was measured with a video camera. The measurement was repeated 3 times for each set of conditions.

(3) Ignition delay time measurement

The ignition delay time was measured changing the concentration of sulfur and temperature in the furnace at atmosphere. The furnace inner diameter was 36 mm, and depth was 36 mm. The furnace bottom temperature was changed from 473 K to 1000 K. The sample weight was about 10 mg and samples were dropped from the upper side of the furnace. After dropping the sample, a blue flame appeared first from the combustion of sulfur, and a luminous flame followed. The time between the drop and appearance of the luminous flame was measured with a high speed video camera. The measurement was repeated 30 times for each set of conditions, and the time for 50% probability of ignition was defined as the ignition delay time.

(4) Temperature measurement near burning surface

The burning rate of BP was very high, and it was difficult to measure the temperature gradient near the burning surface. To measure the temperature gradient, the pressure was set below atmospheric pessure, however at pressures lower than 20 kPa BP did not burn. We measured the temperature gradient to evaluate the effect of sulfur concentration at pressures between 30 kPa and 70 kPa. In this pressure range, burning rate was still high. The pellet was 10 mm in diameter and 10 mm in length and cigarette burning type was used. The line diameter of the thermocouple was 12.5 μm and it was Pt/Pt–10%Rh. The samples were without sulfur (KNO_3/C = 75/15), and with sulfur (KNO_3/C/S = 75/15/10 wt%).

Results and discussion

(1) Thermal decomposition characteristics

Figure 1.1 shows the results of DTA and TG without S (KNO_3/C = 75/15). Without sulfur a large decrease started at 670 K and ended at 760 K and indicated the reaction of black powder. The endothermic peak of KNO_3 appeared at 607 K and was the melting point. The exothermic reaction peak appeared 728 K.

Figure 1.2 shows the results of DTA and TG at ξ_s = 0.25 (KNO_3/C/S = 62.5/12.5/25 wt%). Sulfur melted at 433 K and evaporated at 533 K. The endothermic peak of KNO_3 appeared at 582 K and was the melting point. The exothermic reaction peak appeared at 705 K at ξ_s = 0.25. KNO_3 and S melted at the burning surface. The decomposition temperature decreased with increasing ξ_s.

With sulfur two large decreases appeared: the first decrease started at 433 K and ended at 533 K. The decrease caused by the sulfur evaporation was 20.8% at ξ_s = 0.25 and not all the sulfur content evaporated. Sulfur was considered to exist in the compound generated by the reaction between sulfur and KNO_3 or charcoal. The heat of reaction at the surface was about 2100 kJ kg^{-1} with DSC and also

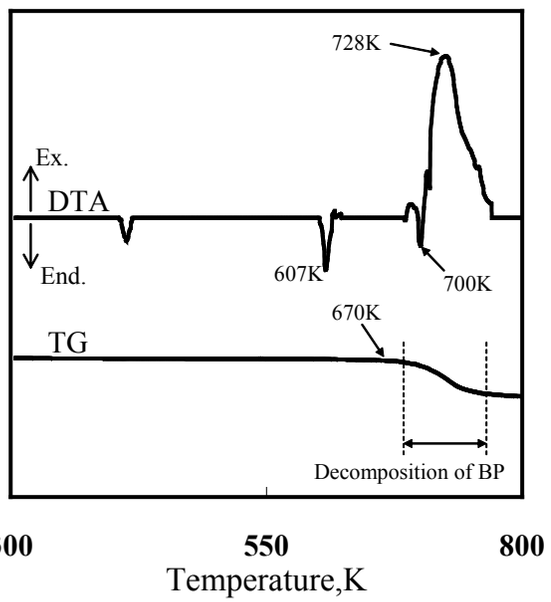

Figure 1.1. *Results of DTA and TG without S.*

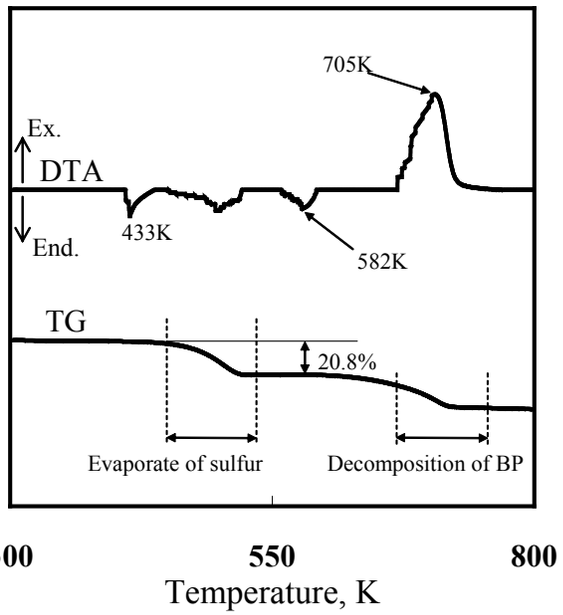

Figure 1.2. *Results of DTA and TG with ξ_s =0.25 (25 wt%).*

did not change with the sulfur concentration.

(2) Burning rate

The relationship between burning rate and concentration of sulfur is shown in Figure 2. The calculated adiabatic flame temperature and *C** are also shown. *C** is the characteristic velocity and is proportional to $T_f^{\frac{1}{2}}$.

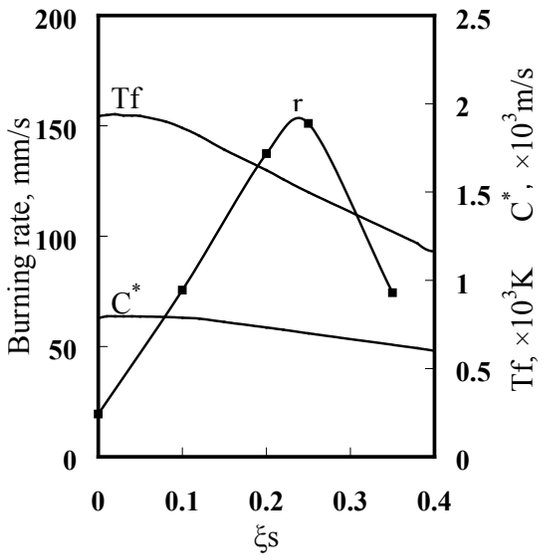

Figure 2. *Burning rate characteristics.*

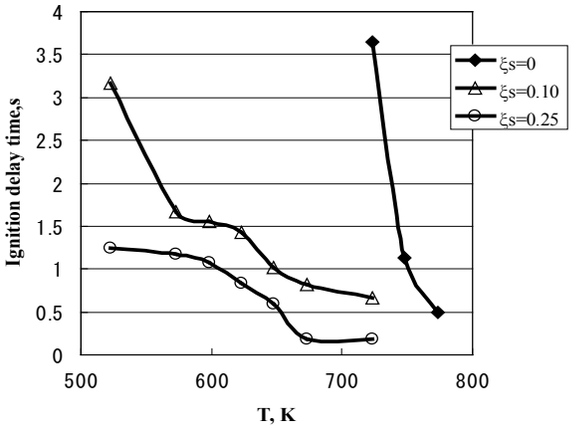

Figure 3. *Ignition characteristics.*

The characteristic velocity was about 787 m s^{-1} which was lower than that of AP composite propellant. The adiabatic flame temperature was over 1500 K at $\xi_s < 0.20$ and the flame temperature was higher than the decomposition temperature. Burning rate increased with increasing ξ_s, and reached a maximum burning rate of 151 mm s^{-1} at $\xi_s = 0.25$. Burning rates were not proportional to the adiabatic flame temperature. Burning rates increased from 2.2 mm s^{-1} to 10.5 mm s^{-1}, when the concentration of oxidizer was changed from 85 wt% to 60 wt% at a ratio of C/S = 15/10. In this case the concentration of sulfur was increased from 6 wt% to 16 wt%. The sulfur melted and evaporated and reacted in the gas phase, therefore these results showed that the heat conducted from the gas phase to the burning surface was an important factor for burning rate.

(3) Ignition characteristics

The relationship between furnace temperature and ignition delay time is shown in Figure 3 at ξ_s = 0, 0.1, 0.25. The concentration of S was 0 (ξ_s = 0), and below 598 K the sample did not ignite. Ignition delay time decreased with increasing furnace temperature and also decreased with increase of concentration of S. These results showed that sulfur affected the ignition delay time.

The ratio of chemical ignition delay time, η_{c*}, is shown in Figure 4 as parameter of ξ_s. The ratio of chemical delay time was smaller than 0.5 at furnace temperature >573 K. The ignition delay time of BP was occupied by physical processes. The ratio of chemical ignition delay time was

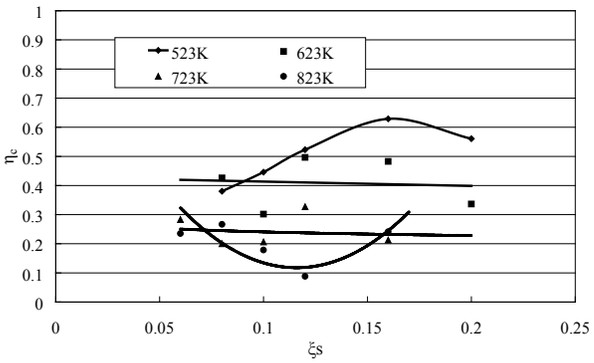

Figure 4. *Ratio of chemical delay time.*

constant at changing sulfur concentration, when the temperature was between 573 K and 773 K. Equation (11) was modified as follows:

$$\tau_c = \alpha \tau_{ig}$$

$$\log \tau_c = \log \alpha + \log \tau_{ig}$$

$$\alpha = \text{constant}$$

$$\log \tau_c \propto \log \tau_{ig} \propto 2 \log \frac{1}{r} \qquad (12)$$

The ratios of τ_c fluctuated when the furnace temperatures were 523 K and 823 K, and so equation (12) could not be used.

(4) Heat balance at burning surface

The temperature profiles near the burning surface were measured with a small thermocouple and are shown in Figure 5. These temperature histories were without S and with ξ_s = 0.1 (10 wt%) at pressure = 30 kPa. Solid phase is shown at distance <0, and zero means at the burning surface. The temperature increased smoothly in the solid phase, and a large variation occurred in the gas phase. The temperature gradients near the burning surface were obtained from these temperature histories. The surface temperature (T_s) and temperature gradient (Φ_{s+}) at 0.1 MPa were estimated from

Table 1. *Surface temperature (T_s), heat of reaction (Q_s), and temperature gradient near burning surface (Φ_{s+})*

Parameter	$\xi_s = 0$	$\xi_s = 0.1$
T_s/K	783	692
Q_s/kJ K^{-1}	2160	2180
$\Phi_{s+} \times 10^3$/K mm^{-1}	5.0	14.8

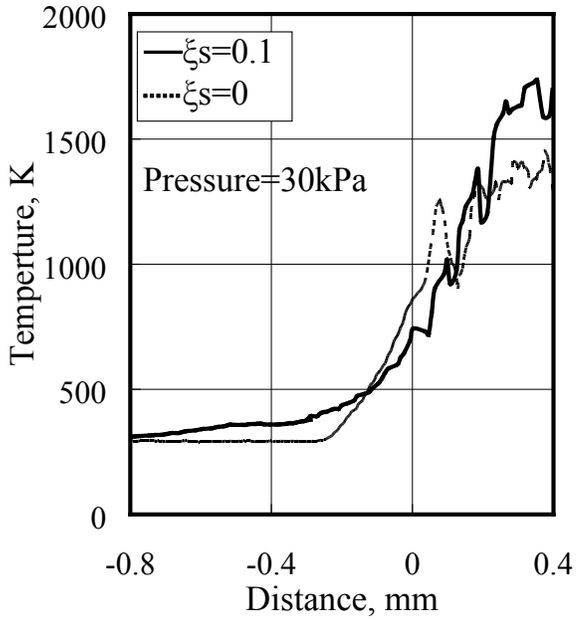

Figure 5. *Temperature histories near burning surface.*

these low pressure values when pressure changed from 30 kPa to 70 kPa. The heat of reaction (Q_s) was obtained with DSC. Surface temperature T_s, Q_s, and Φ_{s+} are shown in Table 1 at a pressure of 0.1 MPa. The surface temperature was 783 K without S, and was 692 K with S and decreased roughly 100 K and the variation was smaller than that of Φ_{s+}. The heat of reaction (Q_s) at the surface was about 2100 kJ kg^{-1} and also did not change with sulfur concentration. The temperature gradient near the burning surface in the gas phase increased with increasing concentration of sulfur. The burning rate was controlled by the reaction rate in the gas phase.

(5) Relationship between burning rate and ignition delay time

The relationship between burning rate and ignition delay time is shown in Figure 6 at 0.1 MPa. The concentration of sulfur changed and the furnace temperature changed from 573 to 823 K. The burning rates were obtained by changing the concentration of sulfur. Ignition delay time and burning rate showed a strong relationship. The burning rate was inversely proportional to the ignition delay time.

The surface temperature T_s and Q_s of BP did not change when the concentration of S changed from

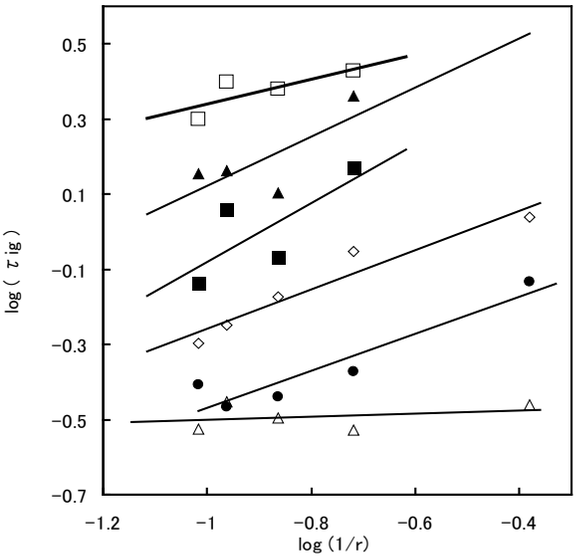

Figure 6. *Relationship between burning rate and ignition delay time.*

0 to10 wt%. It was possible to use equation (4). KNO_3 and S melted at the burning surface, so the physical process time $\tau_{pb} = 0$. The ratio of chemical ignition delay time was constant, when ξ_s was changed from 0 to 20 wt%, so $\tau_c \approx \alpha\tau_{ig}$ was obtained, and it was possible to use equation (12).

Conclusions

The following statements of BP were obtained in this study.

(1) Burning rate increases with increasing sulfur concentration at $\xi_s < 0.25$.

(2) The ignition delay time decreases with increasing furnace temperature and also with increasing S content.

(3) The burning rate is controlled by conductive heat from the gas phase to the burning surface.

(4) The burning rate is inversely proportional to the ignition delay time.

References

1 T. Shimizu, "Studies on Firefly Combustions (Aluminum Charcoal Type)," *Pyrotechnica*, XII June 1988, pp. 7–18.

2 T. Shimizu, *Pyrotechnic Chemistry*, Journal of Pyrotechnics, Inc., 2004, pp. 2.1–2.38.

3 T. Hikita, "Combustion Characteristics and Theoretical Calculation of Black Powder," *Journal of the Industrial Explosives Society, Japan*, Vol. 10, No. 1, 1949, pp. 10–16.

4 S. Hatanaka, "Black Powder for Fireworks," *Japan Explosives Society*, Vol. 11, No. 1, 2001, pp. 2–9.

5 F. A. Williams, "Observations on Burning and Flame-Spread of Black Powder," *AIAA Journal*, Vol. 14, No. 5, 1976, pp. 643–673.

6 N. Kubota, *Rocket combustion*, Nikann Kogyo Press, 1995.

7 N. Kubota, *Propellants and Explosives, Thermochemical Aspects of Combustion*, Wiley-VCH, 2002.

8 S. Gordon and J. B. McBride, *Computer Program for Calculation of Complex Chemical Equilibrium Compositions and Applications*, NASA RP-1311, 1994.

9 H. Abe, M. Tanabe, and T. Kuwahara, "Behavior of Sulfur in Pyrolant for Micro Rocket Motor," *AIAA Paper*, 2004-3725.

10 T. Takeuchi, M. Tanabe, and T. Kuwahara, "The Combustion Characteristics of Black Powder," *33rd International Pyrotechnic Seminar*, 2006, pp. 363–378.